Network Effects on the Nonlinear Rheology of Polymer Nanocomposites

James D. Thomin,[†] Pawel Keblinski,[‡] and Sanat K. Kumar*[,§]

Department of Chemical and Biological Engineering, Rensselaer Polytechnic Institute, Troy, New York 12180; Department of Materials Science & Engineering, Rensselaer Polytechnic Institute, Troy, New York 12180; and Department of Chemical Engineering, Columbia University, New York, New York 10027

Received March 22, 2008
Revised Manuscript Received July 14, 2008

The effect of nanoscale fillers on the mechanical properties of polymers has been extensively studied.[1−14] While there are many interesting aspects to this problem, here we focus on the mechanical behavior of nanocomposites, especially the mechanical reinforcement that is afforded when nanoparticles are added to polymers. The cumulative knowledge in this field points to two primary mechanisms responsible for mechanical reinforcement. The first mechanism, which is essentially particle-driven,[7,15] occurs at relatively high particle volume fraction, beyond the particle percolation threshold, and may be referred to as "jamming". The second, termed the "network reinforcement" mechanism, occurs due to the formation of a long-lived percolating polymer network with the particles as the "network nodes".[11,14,16−18] Recent experiments on pure entangled polymer melts,[19,20] polymers filled with platelet fillers,[3,8,10,21−23] nanotubes,[24] and spherical nanoparticles[16] show that, regardless of reinforcing mechanism, the startup of shear flow is accompanied by stress overshoots. After a certain time, which appears to be related to the "aging" time of the system and the applied strain rate (but not the total strain),[16] the stress recovers to a well-defined plateau value. The viscosities derived from these long-term stress plateaus suggest that these materials shear thin over the whole range of accessible frequencies. Both of these results (i.e., stress overshoots and shear thinning) have been empirically attributed to network structures which exist in the quiescent state, but which are disrupted on the application of shear. While the variation of viscosity with shear flow has been studied through simulations,[6,7,11] simulations have not been used to understand shear stress overshoot on the startup of shear flow.[3,15,16,21]

To gain simulation derived insights into the origins of stress overshoots in the nonlinear rheology of nanocomposites, we perform nonequilibrium molecular dynamics simulations on two different realizations of a quiescent nanocomposite structure possessing the same spatial distribution of nanoparticles. In one case there is a percolating polymer network mediated by the particles, while in the other there is no percolating network present. The transient responses of these two structures to an applied shear are very different and unequivocally show that the percolating structure results in stress overshoots. Detailed analysis demonstrates that only the polymer strands which "bridge" the particles to form a percolating network experience stress overshoots, with these overshoots disappearing when the network is broken. While the time needed to break this transient network increases with decreasing strain rate, the net strain at the maximum stress overshoot value is approximately constant with strain rate. Finally, we make connections between these results and those obtained from solutions of entangled polymers and suggest that the origins of stress overshoot in those cases also arise from a network of transient physical cross-links.

The equilibrium simulation model has been described in detail in our previous work.[18] In brief, the simulation cell is a cubic box with side length of $\sim 18\sigma$, resulting in a reduced monomer density of 0.85, which is representative of a polymer melt. Periodic boundary conditions are used in all three spatial directions. The box contains 60 Kremer−Grest[25] polymer chains with degree of polymerization $N = 80$ (with rms radius of gyration, $R_g \sim 4.7\sigma$): this chain length is in the crossover regime between Rouse and reptation dynamics. All of the polymer monomers interact with a Lennard-Jones (LJ) potential, $U(r) = 4\varepsilon[(\sigma/r)^{12} - (\sigma/r)^6]$, which has been truncated at its minimum $r = 2^{1/6}\sigma$ and shifted so that both the potential and the force go to zero at the cutoff.[26] Adjacent chain monomers are bonded by a FENE potential: $V_{FENE} = -k(R_0^2/2)\ln(1 - (r/R_0)^2)$, with $k = 30\varepsilon/\sigma^2$ and $R_0 = 1.5\sigma$.[25] The polymer melt surrounds four roughly spherical particles with radius $R_p \sim 5\sigma$; each particle consists of 116 monomers which are identical to the polymer monomers but arranged in an FCC configuration maintained by FENE bonds connecting nearest neighbors.[25] The attractive polymer−particle interactions are described by a shifted-force LJ potential[26] with a cutoff of $r = 1.5\sigma$ and $\varepsilon = 20$. All production runs were conducted in the NVT ensemble, using a simple velocity rescaling thermostat with $T^* = kT/\varepsilon = 1$ in Lennard-Jones reduced units.[27] The equations of motion were integrated using the velocity-Verlet algorithm,[27] with time step $d\tau = 0.005$ (in reduced LJ units). Shear was applied through simple Lees−Edwards boundary conditions.[27] A typical simulation run consisted of 50×10^6 time steps ($250\,000\tau$). Stress measurements were taken every 10 time steps, and trajectory snapshots for structural calculations were saved every 10 000 time steps. Stress was calculated using the atomic virial definition:[27]

$$-\sigma_{\alpha\beta} = P_{\alpha\beta} = \frac{1}{V}\left(\sum_i p_{i\alpha}p_{i\beta}/m_i + \sum_i \sum_{j>i} r_{ij\alpha}f_{ij\beta}\right) \qquad (1)$$

where $\alpha \neq \beta$ indicates the vector components along the three spatial directions, the subscripts i and j are atomic indices, p is momentum, m is mass, r is the pair radial separation, and f is the pair force. The off-diagonal elements of the stress tensor were recorded every 10th time step. In sheared runs, the stress was averaged over time blocks of 10^6 time steps (5000τ) for the time-dependent stress plots. Viscosity was calculated using[27] $\langle\sigma_{xy}\rangle = \eta\dot{\gamma}$ with the stress being averaged over the entire run after the steady state has been attained (i.e., the initial response has decayed). For equilibrium simulations, the autocorrelation function of the off-diagonal elements of the stress tensor was calculated using the fast Fourier transform method:[27] $G(t) = \langle\sigma_{\alpha\beta}(t)\,\sigma_{\alpha\beta}(0)\rangle$ where the brackets denote an ensemble average over starting times. This corresponds to the time-dependent modulus, $G(t)$, that would be measured in a stress relaxation experiment (stress relaxation function). A more detailed description of the stress calculations, including our

* Corresponding author. E-mail: sk2794@columbia.edu.
[†] Department of Chemical and Biological Engineering, Rensselaer Polytechnic Institute.
[‡] Department of Materials Science & Engineering, Rensselaer Polytechnic Institute.
[§] Columbia University.

10.1021/ma8006398 CCC: $40.75
Published on Web 07/26/2008

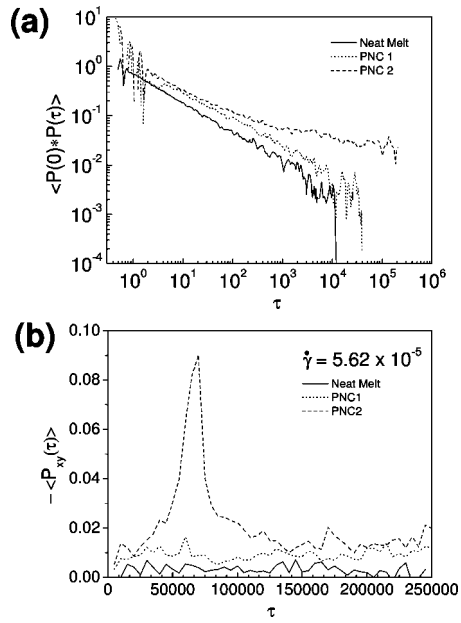

Figure 1. (a) Stress relaxation functions for quiescent melts **PNC1** (dotted line), **PNC2** (dashed line), and neat melt (solid line). (b) Stress vs time for **PNC1** (dotted line), **PNC2** (dashed line), and neat melt (solid line), at a shear rate of 5.62×10^{-5}. Reduced LJ units are used in both figures.

method of smoothing and truncating the stress relaxation functions, can be found in our previous work.[28]

At this level of polymer−particle attraction, an essentially glassy layer of polymer segments is bound to the surface of the particles. Therefore, differences in system preparation can lead to structural differences, which consequently lead to differences in the stress response, as shown in ref 18. In this work, we studied systems prepared by two different methods: **PNC1** structures were created by generating 15 chains using a self-avoiding random walk at low density (∼0.1) around a single particle, then reproducing this structure four times in an FCC configuration, and compressing the entire system to a reduced melt density of 0.85 using an NPT simulation run. During this compression, the attractive interactions between polymer and particles were "turned on". **PNC2** structures were created by generating the four particles in an FCC configuration and then placing all the chains side-by-side in a linear configuration, again at low density. The system was then compressed using an NPT run to a melt density of 0.85 and fully equilibrated, *before* attractions were turned on. Our models are not in true equilibrium and hence the particles are not diffusive, and chains that are bonded to the particles are also not diffusive. In general, **PNC1** structures have a relatively small number of chains bonded to a particle, and these chains tend to wrap around the particles rather than bridge between particles. **PNC2** structures have more chains bonded to particles and have a greater number of bridging chains. As we will show below, this results in significantly different stress responses in the two systems.

We now consider the quiescent stress response of these systems (Figure 1a). The **PNC1** structure, without a percolating network, shows an overall increase in the stress relaxation function relative to the neat melt, although their temporal evolutions are qualitatively similar. This indicates a uniform increase or "renormalization" of the Rouse relaxation times of the polymer chains.[18] **PNC2**, characterized by a percolating network, clearly shows solidlike behavior at long times, indicating a new relaxation mechanism in addition to the renormalization of Rouse times. This plot also demonstrates that the systems have not reached a true equilibrium, since ensemble averages of equilibrated systems would give identical (within error) stress ACF curves.

Figure 1b shows the stress response to the constant rate shear as a function of time for the lowest shear rate studied (5.62×10^{-5}). Clearly, **PNC2** (reinforced) shows a buildup of the stress as the deformation increases. The stress reaches its maximum magnitude and then decays to a steady-state value. This long time plateau value is precisely the same as the steady-state value of the stress for **PNC1** (nonreinforced). Note, however, that the **PNC1** structure does not exhibit a stress overshoot at all. This result clearly establishes that the network which reinforces **PNC2** is broken at sufficiently large strain and is not reestablished (see more on this below). After this time both systems show the same stress response implying that memory effects are eliminated by the deformation process.

An important caveat here is the role of the algorithm used to simulate the system. We have used Lees−Edwards boundary conditions, where shear is imposed at the surfaces of the cell. The velocity profiles evolve from the surface into the middle of the simulation cell with increasing run time. It is important to know whether the **PNC2** network was broken during the evolution of this velocity profile or after a "steady-state" velocity profile had been attained. We have examined the velocity profiles and found that the network "breaks" before the steady-state velocity profile is attained for one of the largest shear rates (1×10^{-3}) used. The results for a shear rate that is 1 order of magnitude lower are unclear: the velocity profiles are too noisy to definitively draw any conclusion. While a different algorithm such as SSLOD may help to resolve this issue, we note that the fact which remains is that the major difference between **PNC1** and **PNC2** is the existence of a network in the latter, which breaks under the action of shear.

For different shear rates the peak stress response occurs at different times. Figure 2a shows that this peak occurs in a narrow range of total strain values (6−8). It also appears that the strain at which the stress reaches its peak value increases with increasing shear rate. However, detailed analysis of all strain rates studied (not just the three shown here) indicates that this is more closely related to the specifics of the network than to the strain rate. In some cases the peak time increases with strain rate, and in others it decreases, but on average, there is no measurable correlation. The steady-state value of the stress allows us to calculate the nanocomposite viscosity (Figure 2c). The first observation is that the viscosities of the two composite systems are essentially identical. This again demonstrates that the shear leads, at long enough times, to a unique steady state independent of the initial network structure. The comparison with the results for the neat melt yields additional insights. At high shear rates, the nanocomposite systems exhibit a uniform increase in viscosity relative to the neat melt. This behavior is consistent with the picture of a renormalization of the Rouse relaxation times in systems without reinforcing networks.[7,18] At lower shear rates, the neat melt reaches the rate-independent Newtonian regime, with a zero shear-limit viscosity value that is the same as that obtained in equilibrium MD simulations. By contrast, as the shear rate increases, the viscosity of the nanocomposites continuously decreases. This simply means that the onset of shear thinning in composites occurs at much lower shear rates than in neat melts. This observation is consistent with the longer relaxation times present in the composites, which are associated with chain immobilization at the polymer−nanoparticle interfaces. We note that we were unable to further

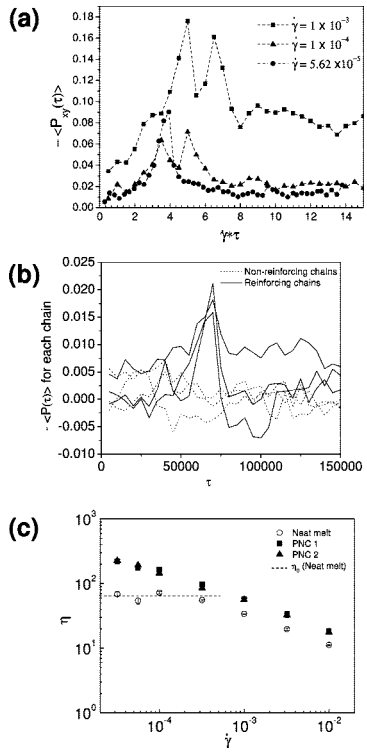

Figure 2. (a) Stress response of **PNC2** for shear rates of 1×10^{-3} (squares), 1×10^{-4} (triangles), and 5.62×10^{-5} (circles) plotted as a function of total strain. (b) Stress for individual chains vs time for **PNC2** for a shear rate of 5.62×10^{-5}. Each line represents one of the 60 chains in the system. For clarity, only three nonreinforcing chains (dotted lines) are shown in addition to the three reinforcing chains (solid lines). (c) Viscosity vs shear rate for **PNC1** (squares), **PNC2** (triangles), and neat melt (open circles). The dashed line indicates the viscosity of the neat melt obtained from equilibrium MD simulations[28] (also see Figure 1). Reduced LJ units are used in all figures.

explore the issue of shear thinning due to computational limitations which prevent us from studying lower shear rates.

While it is evident from Figures 1b and 2a that there is mechanical yielding in network reinforced systems, a clear understanding of the network breakage requires a more detailed analysis. First, in addition to the overall shear stress, we monitored the shear stress for individual chains using the virial stress definition (eq 1). The chain stress for the shear rate shown in Figure 1b is plotted as a function of time for several chains in Figure 2b. Surprisingly, we found that only three chains were supporting the excess stress developed about the yielding point. Furthermore, an analysis of the chain end-to-end distance shows no signature of yielding for any chains. A closer look at the microstructure of the system offers insights into these observations. In **PNC1** there are 6−8 chains bridging between particles on average, but only three of these persist for the entire simulation. Furthermore, these three chains do not form a percolating network across the simulation cell. In the case of the reinforced system, there are 12−20 bridging chains on average, and a percolating network exists which consists of 12−16 persistent bridges connecting all of the particle pairs. In general, if a polymer chain only makes contact with the particle through one or two monomers, the bridge will not persist. Above a certain critical threshold, which we estimate at ∼5 monomers the bridge will persist for the entire simulation. As the network is strained, the shortest path through the network is stressed. At this shear rate (5.62×10^{-5}), the shortest path is represented by three chains. As the strain increases, many chains in the system are extended, but only these three chains are

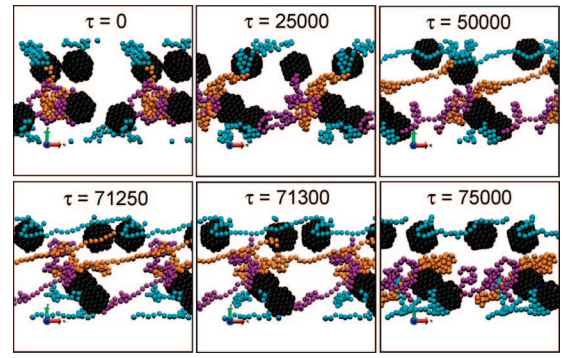

Figure 3. Simulation snapshots of the three reinforcing chains in PNC2 at a shear rate of 5.62×10^{-5}. Periodic images in the $+x$ and $-x$ directions are shown along with the central simulation box. The velocity gradient is in the y direction. The perspective is looking down the z-axis. The orange chain is stretched until it detaches from one particle at $t \sim 71\,300$, allowing all the previously stretched bridges to relax. Pictures were generated using Visual Molecular Dynamics (VMD) software.[31]

extended enough to lead to bond stretching. Since only relatively small lengths of these particular chains form bridges (10−20 monomers), there is no sign of this stretching in the end-to-end distance calculation. Eventually, the strain energy overcomes the entropic spring force, and the bridges become fully extended. At this point, bond stretching occurs, leading to the increase in stress. The stress continues to build until the bond stretching energy becomes greater than the energy binding the polymer to the particles. This binding energy is related to the potential energy well depth, the number of monomers attached to the surface, and the orientation of those monomers. Once the binding energy is surpassed, the chain monomers begin to "peel off" of the particle surface, until the entire chain has detached. The other bridges remain intact and subsequently relax (Figure 3). For this particular network and shear rate, breaking a single bridge destroys the percolating network.

We note three important differences between the stress behavior observed in this work and those reported in the literature.[16] The first is that we see multiple peaks in the stress overshoot at high shear rates, while experimentally only a single peak is seen. Despite the fact that all **PNC2** runs were started from the same configuration, at higher shear rates, it takes multiple bridge breaks before the network is destroyed. This could be due to the fact that at lower shear rates the chains have the ability to relax before the network is fully strained and will therefore align so that the network strain is minimized. At faster strain rates, the network does not have time to change before stress begins to build. The shortest path through the network in these cases consists of bridges of varying lengths. Thus, we see multiple yield points. The second difference between the stress overshoots seen in this work and those seen experimentally is that in real systems the time of the peak does not depend simply on strain rate or on total strain,[16] but instead follows a power law where $t_{peak} \sim (d\gamma/dt)^{-0.5}$. In our case, the peak times are very close to constant with total strain. Finally, we note that when the yield stress of the composite system is calculated by fitting our data via the Casson equation[29] $\sqrt{\sigma} = \sqrt{\sigma_0} + \beta\sqrt{\dot{\gamma}}$ (where σ is the steady-state stress, σ_0 is the yield stress, and β is an arbitrary constant), we obtain a value of ∼0.002, ∼1 order of magnitude lower than the plateau modulus ($G_{plateau} \sim 0.02$) from our quiescent simulations. This is in qualitative agreement with what is observed experimentally, with the rationalization that the network structure which is responsible for the stress overshoots is broken during steady shear but

remains intact in quiescent simulations and low-amplitude oscillatory shear experiments. However, the results are quantitatively different, since in experiments the yield stress was 3 orders of magnitude lower than the limiting value of the complex modulus as the complex viscosity approached infinity.[16] We hypothesize that all of these differences are an artifact of our small system size and that if we were able to simulate much larger systems, or alternatively average many realizations of small systems, we would see a large distribution of yield points manifested in a broad, smooth peak, with a peak time dependence on shear rate similar to what is observed experimentally. Furthermore, in a larger system we would expect to see much more network structure, leading to a higher plateau modulus. Since the steady-state stress is not dependent on interparticle network structure, the yield stress obtained via the Casson equation would remain the same, and the resulting difference in magnitudes would be in closer qualitative agreement with experiments. In any case, it is clear that more work is required to understand these differences.

Our results unequivocally show that an interparticle polymer network is responsible for the stress overshoots seen in our simulations. This observation has far-reaching significance and can be used to better understand results which are well-known in the experimental literature. Stress overshoots have been seen both in pure entangled polymers[20,30] and in filled polymer systems.[3,8,10,16,21–24] In each of these cases the molecular nature of the network is obviously different, e.g., physical entanglements between pure polymers vs particles acting as nodes in a filled system. Despite differences in system specifics, our work points to a universal underlying requirement: for stress overshoots to occur, a percolating network of some kind must exist.

References and Notes

(1) Ganesan, V.; Pryamitsyn, V.; Surve, M.; Narayanan, B. *J. Chem. Phys.* **2006**, *124*, 221102.
(2) Havet, G.; Isayev, A. I. *Rheol. Acta* **2003**, *42*, 47.
(3) Hsieh, A. J.; Moy, P.; Beyer, F. L.; et al. *Polym. Eng. Sci.* **2004**, *44*, 825.
(4) Krishnamoorti, R.; Vaia, R. A.; Giannelis, E. P. *Chem. Mater.* **1996**, *8*, 1728.
(5) Mackay, M. E.; Dao, T. T.; Tuteja, A.; et al. *Nat. Mater.* **2003**, *2*, 762.
(6) Pryamitsyn, V.; Ganesan, V. *J. Rheol.* **2006**, *50*, 655.
(7) Pryamitsyn, V.; Ganesan, V. *Macromolecules* **2006**, *39*, 844.
(8) Ren, J. X.; Krishnamoorti, R. *Macromolecules* **2003**, *36*, 4443.
(9) Smith, G. D.; Bedrov, D.; Li, L. W.; et al. *J. Chem. Phys.* **2002**, *117*, 9478.
(10) Solomon, M. J.; Almusallam, A. S.; Seefeldt, K. F.; et al. *Macromolecules* **2001**, *34*, 1864.
(11) Starr, F. W.; Douglas, J. F.; Glotzer, S. C. *J. Chem. Phys.* **2003**, *119*, 1777.
(12) Surve, M.; Pryamitsyn, V.; Ganesan, V. *J. Chem. Phys.* **2006**, *125*, 064903.
(13) Xu, L.; Reeder, S.; Thopasridharan, M.; et al. *Nanotechnology* **2005**, *16*, S514.
(14) Zhang, Q.; Archer, L. A. *Langmuir* **2002**, *18*, 10435.
(15) Zhu, Z. Y.; Thompson, T.; Wang, S. Q.; et al. *Macromolecules* **2005**, *38*, 8816.
(16) Goel, V.; Chatterjee, T.; Bombalski, L.; et al. *J. Polym. Sci., Part B: Polym. Phys.* **2006**, *44*, 2014.
(17) Salaniwal, S.; Kumar, S. K.; Douglas, J. F. *Phys. Rev. Lett.* **2002**, *89*, 258301.
(18) Sen, S.; Thomin, J. D.; Kumar, S. K.; et al. *Macromolecules* **2007**, *40*, 4059.
(19) Tapadia, P.; Wang, S. Q. *Phys. Rev. Lett.* **2006**, *96*000.
(20) Wang, S. Q.; Ravindranath, S.; Boukany, P.; et al. *Phys. Rev. Lett.* **2006**, *97*000.
(21) Lele, A.; Mackley, M.; Galgali, G.; et al. *J. Rheol.* **2002**, *46*, 1091.
(22) Treece, M. A.; Oberhauser, J. P. *Polymer* **2007**, *48*, 1083.
(23) Treece, M. A.; Oberhauser, J. P. *Macromolecules* **2007**, *40*, 571.
(24) Abdel-Goad, M.; Potschke, P. *J. Non-Newtonian Fluid Mech.* **2005**, *128*, 2.
(25) Kremer, K.; Grest, G. S. *J. Chem. Phys.* **1990**, *92*, 5057.
(26) Stoddard, S. D.; Ford, J. *Phys. Rev. A* **1973**, *8*, 1504.
(27) Allen, M. P.; Tildesley, D. J. *Computer Simulation of Liquids*; Oxford University Press: Oxford, 1987.
(28) Sen, S.; Kumar, S. K.; Keblinski, P. *Macromolecules* **2005**, *38*, 650.
(29) Malkin, A. Y. *Adv. Polym. Sci.* **1990**, *96*, 69.
(30) Wang, S. Q. *Macromol. Mater. Eng.* **2007**, *292*, 15.
(31) Humphrey, W.; Dalke, A.; Schulten, K. *J. Mol. Graphics* **1996**, *14*, 33.

MA8006398